Atomic and Nanoscale Spin Dynamics

R. Skomski, A. Ullah, B. Balasubramanian and D. J. Sellmyer

Department of Physics and Astronomy and Nebraska Center for Materials and Nanoscience, University of Nebraska, Lincoln, NE 68588

Abstract

The relationship between quantum mechanics and nanoscale spin dynamics is investigated by analyzing past work in magnetism and beyond. Findings about magnetization dynamics, accumulated throughout the 20th century, are revisited from a unifying modern perspective and related to trends in other areas of physics and technology. Traditional topics, for example spin precession and thermally activated magnetization processes, are discussed with emphasis on characteristic times and length scales, showing that nanoscale magnetization dynamics is very different from atomic spin dynamics. It is shown how these topics are connected to more recent developments such as the Berry phase, the no-cloning theorem, quantum-spin fluctuations, and THz magnetization dynamics in antiferromagnets.

1. Introduction

The temporal evolution of spin structures is one of most intriguing aspects of magnetism. Dynamic effects cover many orders of magnitude, from femtosecond atomic processes to millions of years in rock magnetism, with applications ranging from ultrafast data processing in computers and microwave to long-time data storage in magnetic recording. The observation of magnetic viscosity in 1893 [1] may be considered the starting point of the investigation of materials-specific magnetization dynamics, preceded by Foucault's 1855 discovery of eddy currents [2]. Milestones in the first half of the 20th century were Bloch's work on spin waves (magnons) [3], the 1935 paper by Landau and Lifshitz, which deals with domain formation and micromagnetic dynamics [4], and the explanation of magnetic viscosity by Becker and Döring in 1939 [5]. More recent developments are the Berry phase [6] and the no-cloning theorem [7, 8].

The time-dependent Schrödinger equation predicts $\Delta E = \hbar\omega$, that is, large energy differences corresponds to fast processes. The characteristic times $\tau_o = 1/f$ are $2\pi\hbar/\Delta E$, meaning that small energy-level spacings correspond to slow quantum mechanics. Magnetic interaction energies are typically below 0.1 meV and tend to yield frequencies f of several GHz. For comparison, the current-based ENIAC computer of 1945 had a clock speed of 0.1 MHz, whereas clock rates of current PCs are a few GHz. Interatomic exchange is stronger by roughly three orders of magnitude and corresponds to several THz. Such high frequencies are observed in antiferromagnets and attractive for ultrafast information processing [9].

The huge differences in frequencies reflect the distinction between relativistic and nonrelativistic interactions, epitomized by Zeeman and exchange energies, respectively. Relativistic interactions are weaker by a factor of α^2, where $\alpha = 1/137$ is Sommerfeld's fine-structure constant, and yield much slower dynamics. Intra-atomic exchange is typically about 1 eV, corresponding to $f = 242$ THz and $t_o = 0.414$ fs, meaning for example that intra-atomic spin dynamics is almost femtosecond. Multiplication by a^2 yields 12.88 GHz, of the order of magnitude typically encountered in ferromagnetic resonance.

Artificial or natural nanostructuring plays an important role in the understanding and exploitation of magnetization dynamics. While quantum-mechanical processes dominate on an atomic length scale, nanoscale dynamics is qualitatively different. For example, the Schrödinger equation is reversible, that is, for each process going forward in time there is a process going back, whereas nanoscale and macroscopic processes are irreversible. In real space, α yields a typical length scale of $a_o/\alpha = 7.252$ nm [10, 11], which also hints at the importance of nanoscale length considerations in spin dynamics.

This paper summarizes the basic physics of nanoscale spin dynamics, starting with early 20th century and including recent findings. Emphasis is on the interplay of the different quantum-mechanical and thermodynamic mechanisms.

2. Time-dependent quantum mechanics

The zero-temperature time dependence of a physical system is governed by the action $\mathcal{S} = \int \mathcal{L}\, dt$, where $\mathcal{L}$ is the Lagrangian. Classically, the evolution of the system is an extremum of $\mathcal{S}$, whereas quantum-mechanically, it involves fluctuations around the extremal path. The Lagrangian can be written as $\mathcal{L} = X\,P - \mathcal{H}$, where $\mathcal{H}$ is the Hamiltonian and X and P are generalized coordinates and momenta, respectively. The distinction between $\mathcal{L}$ and $\mathcal{H}$ is important in periodic and curved spaces (§2.3).

2.1. Equation of motion

Let us, for the moment, assume that the dynamics is exclusively determined by the Hamiltonian, through the Schrödinger equation $i\hbar\partial\psi/\partial t = \mathcal{H}\psi$. The focus is normally on time-independent operators A, such as the spin contribution $\mathbf{S} = ½\,\boldsymbol{\sigma}$ to the magnetization M, where $\boldsymbol{\sigma}$ is the spin vector containing the Pauli matrices σ_x, σ_y, and σ_z. Quantum-mechanical averages

$$<\mathrm{A}(t)> = <\psi(t)|\mathrm{A}|\psi(t)> \tag{1}$$

are obtained in a conceptually straightforward way from wave function $|\psi(t)>$, but this approach is often cumbersome. It is more convenient to construct *equations of motion* for $<\mathrm{A}>$. Taking the time derivative of Eq. (1) and using the Schrödinger equation lead to

$$\frac{\mathrm{d}<\mathrm{A}(t)>}{\mathrm{d}t} = \frac{\mathrm{i}}{\hbar} <\psi(t)|\mathcal{H}\mathrm{A} - \mathrm{A}\mathcal{H}|\psi(t)> \tag{2}$$

Consider an electron in an external magnetic field H, described by the Zeeman interaction $\mathcal{H} = -\mu_o\mu_B M_s \boldsymbol{H}\cdot\boldsymbol{\sigma}$. To obtain the equation of motion for the three spin components, $\mathrm{A}_i = (S_x, S_y, S_z)$, we put A_i and $\mathcal{H}$ into Eq. (2). This yields matrix products of the type $\sigma_i\,\sigma_j$, which are simplified by exploiting that Pauli matrices obey cyclic relations such as a $\sigma_x\,\sigma_y = -\sigma_y\,\sigma_x = i\sigma_z$. Collection of all products in Eq. (2) then yields the equation of motion

$$\mathrm{d}\langle \mathbf{S} \rangle/\mathrm{dt} = \gamma_o \langle \mathbf{S} \rangle \times \boldsymbol{H} \tag{3}$$

where $\gamma_o = 2\mu_o\mu_B/\hbar = \mu_o e/m$. This equation is a spin-precession analog to the Larmor precession, which reflects the orbital motion of electrons.

A quasiclassical version of Eq. (3) is

$$\mathrm{d}\boldsymbol{M}/\mathrm{dt} = \gamma_o \boldsymbol{M} \times \boldsymbol{H} \tag{4}$$

where $\boldsymbol{H}$ is actually an effective field that includes demagnetizing-field and magneto-crystalline anisotropy contributions, such as $H_A = 2K_1/\mu_o M_s$ [12, 13]. When the x and y directions are inequivalent, then one needs to explicitly consider two equations for M_x and M_y. This case is exemplified by a ferromagnetic slab having dimensions $L_x \neq L_y \ll L_z$, which exhibits two different demagnetizing factors in the x- and y-directions, corresponding to effective fields $H_x \neq H_y$ and resonance frequencies $\omega_x \neq \omega_y$ [12, 13, 14]. In a strict sense, the effective field also includes exchange fields $\boldsymbol{H}_{ex} = \lambda \boldsymbol{M}$, which are very strong (up to several 100 T), but since $\boldsymbol{M} \times \boldsymbol{M} = 0$, the contribution can be ignored.

Equations (4-5) mean that high fields lead to fast dynamics, which is important, for example, in magnetic data processing. The numerical value of γ_o is almost exactly 28 GHz per tesla. Fields of more than 1 T are difficult to create, especially in miniaturized devices, which makes the THz information processing a challenge (§5.3).

2.2. Nonzero temperatures

Equation (2) can be simplified by introducing the Liouville operator L [15, 16]

$$\mathsf{L} = (\mathrm{i}/\hbar)\,(\mathcal{H}\mathsf{A} - \mathsf{A}\mathcal{H}) \tag{5}$$

which is actually a "superoperator", because it acts on another operator, not on a wave functions. Equation (5) is very useful in the description of finite-temperature dynamics. At nonzero temperatures, different quantum states ψ_μ are occupied, so that Eq. (1) must be replaced by

$$\langle \mathsf{A}(t) \rangle = \Sigma_\mu\, p_\mu \langle \psi_\mu(t)|\mathsf{A}|\psi_\mu(t)\rangle\ . \tag{6}$$

In terms of the eigenvalues E_μ of the Hamiltonian, the equilibrium probabilities are $p_\mu \sim \exp(-E_\mu/k_BT)$. In the nonequilibrium case, one has some distribution $p_\mu(0)$ and needs to separately consider each wave function $\psi_\mu(t)$. A simple example will be discussed in §3.2.

Th use of wave functions can be avoided by rewriting Eq. (6) as $\langle \mathsf{A}(t) \rangle = \mathrm{Tr}\,(\mathsf{A}\,\rho(t))$, where ρ is the density matrix [16]. In equilibrium, $\rho \sim \exp(-\mathcal{H}/k_BT)$, whereas non-equilibrium density matrices obey the equation $\rho(t) = \mathrm{e}^{-t\mathsf{L}}\,\rho(0)$. The practical challenge is that $\mathcal{H}$ and therefore L contains a heat-bath degree of freedom (§4).

2.3. Berry phase

The $X\,P$ term in the Lagrangian can be ignored in the case of linear motion, where $\mathcal{L}$ and $\mathcal{H}$ yield the same dynamics. However, $\mathcal{L}$ is more fundamental than $\mathcal{H}$, and the difference is important, for curved and cyclic geometries, where it corresponds to the *Berry phase* γ [6, 17, 18, 19]. In this case, the wave function ψ in the Schrödinger equation must be replaced by $e^{i\gamma}\psi$. The Berry phase is unrelated to the Hamiltonian and to its energy eigenvalues but nevertheless affects the motion of electrons. Examples in nanomagnetism are the Aharonov-Bohm and topological Hall effects [17, 18]. In fact, even the ordinary precession of electron spins $\mathbf{S} = ½\,\boldsymbol{\sigma}$ involves a Berry phase, because the Bloch sphere hosting the vector $\boldsymbol{\sigma}$ is a curved space.

The topological Hall effect is caused by conduction electrons rotating through exchange interactions with noncoplanar localized spins, for example in magnetic skyrmions [18, 19]. The kinetic energy of the conduction electrons is described by the operator $-(\hbar\,/2m_e)\nabla^2$, which acts on the wave function $e^{i\gamma}\psi$. The identity

$$\nabla^2(e^{i\gamma}\psi) = e^{i\gamma}(\nabla + i\nabla\gamma)^2\psi \tag{7}$$

moves the term $e^{i\gamma}$ to the left of the nabla operators, leading to $\psi^* e^{-i\gamma} e^{i\gamma}\psi = \psi^*\psi$. However, this procedure produces a magnetic vector potential $\boldsymbol{A} \sim \nabla\gamma$ and yields an emergent magnetic field $\boldsymbol{B} = \nabla \times \mathbf{A}$ that contributes to the Hall effect.

2.4. The no-cloning theorem

Some aspects of nanomagnetism are quasi-classical, that is, quantum fluctuations are of secondary importance. For example, bits of information stored in magnetic recording media are classical, because they can assume two values only, such as $\boldsymbol{M} = \pm M_s\,\mathbf{e}_z$. By comparison, quantum bits (qubits) correspond to vectors on a Bloch sphere and have components in all three spin directions [20].

Exploiting these quantum-mechanical degrees of freedom information processing has remained a challenge. One aspect is the need to copy quantum bits, for example for error correction. The *no-cloning theorem* states that it is impossible to create an identical copy of an unknown quantum state $|\psi\rangle$ [7, 8, 20], in striking contrast to classical information.

The aim of cloning is to start from $|\psi\rangle$ and to create a quantum state $|\psi\rangle|\psi\rangle$. Alternatively, one can start from $|\psi\rangle\,|0\rangle$, where $|0\rangle$ is known and therefore uninteresting. Let us assume that there is a unitary operator $\mathcal{U}$ with cloning ability, meaning that $\mathcal{U}|\psi\rangle|0\rangle = |\psi\rangle|\psi\rangle$ and $\mathcal{U}|\phi\rangle|0\rangle = |\phi\rangle|\phi\rangle$. Multiplication of $\langle\psi|\langle 0|\,\mathcal{U}^+ = \langle\psi|\langle\psi|$ and $\mathcal{U}\,|\phi\rangle|0\rangle = |\phi\rangle|\phi\rangle$ yields $\langle\psi|\phi\rangle = \langle\psi|\phi\rangle\,\langle\psi|\phi\rangle$. This quadratic equation for $\langle\psi|\phi\rangle$ is of the type $x = x^2$ and has two solutions, namely $\langle\psi|\phi\rangle = 0$ (orthogonal states) and $\langle\psi|\phi\rangle = 1$, or $|\psi\rangle = |\phi\rangle$. In other words, while classical bits (binary values 0 and 1) can be copied easily, the cloning of quantum bits is impossible.

The no-cloning theorem is important in many areas of quantum computing. For example, it excludes the use of entangled Bell quantum states such as $|\uparrow\rangle|\downarrow\rangle - |\downarrow\rangle|\uparrow\rangle$ for faster-than-light communication [8, 20]. Long-distance entanglement can be realized conceptually very easily by increasing the distance between two atoms in a hydrogen molecule, but such a long-distance entanglement is susceptible to environmental perturbations and sluggish to manipulate, because t_o is inversely proportional to the hopping integral and therefore increases exponentially with interatomic distance.

Much work has been done since the 1980s to develop approximate cloning procedures, realized for example through iteration [20]. The no-cloning problem does not occur in the copying of biological information, where the information is stored in form of atomic positions in the DNAs. Atoms are much heavier than electrons, so their de-Broglie wavelength $\lambda_B \sim 1/m$ is far too small to interfere with the atomic positions and the information is stored classically. Quantum effects are important for the *electrons* in the DNA, but they merely ensure chemical bonding.

3. Transition to nanoscale dynamics

The Schrödinger equation is reversible, Fig. (1a), in contradiction to experiment. One example is the phenomenon of damping, where an out-of-equilibrium system relaxes back to equilibrium, Fig. 1(b). The time-dependent many-body Schrödinger equation can be used to predict the evolution of any nanoscale or macroscopic system, but this is neither practical nor necessary, because individual heat-bath degrees of freedom do not contain relevant magnetic information. Relaxation is, in fact, caused by the averaging over the irrelevant degrees of freedom [15]. This coarse-graining procedure yields equations of motion for the relevant magnetic degrees of freedom, such as the position of a domain wall.

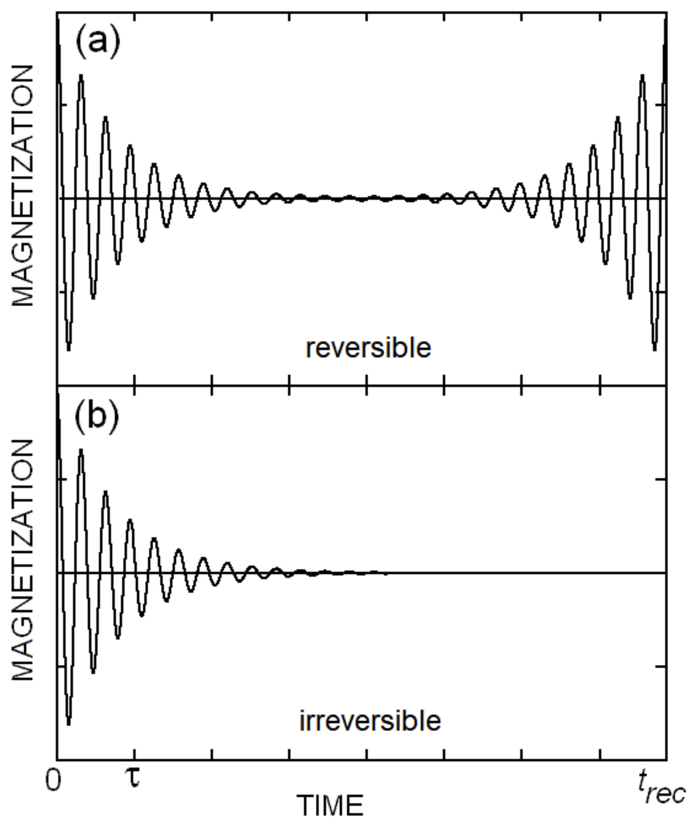

Fig. 1. Irreversibility: (a) Zermelo's recurrence paradox and (b) experimentally realized situation (damping).

3.1. Recurrence paradox

Quantum states predicted by the Schrödinger equation are quasi-periodic, the original state being recovered after some time, Fig. 1(a). This is known as Zérmelo's recurrence paradox [15]. Furthermore, the Liouville operator does not change the entropy $k_B<\ln\rho>$, because it conserves the phase-space volume. This conservation is illustrated by Gibb's ink parable, where a droplet of immiscible ink is stirred into a liquid (Fig. 2). As one goes from the top left to the bottom right of the figure, the ink becomes more and more evenly distributed, but the entropy does not increase.

The recurrence paradox is solved by distinguishing between relevant and irrelevant degrees of freedom. The local magnetization $\boldsymbol{M}(\boldsymbol{r})$ is a typical relevant degree of freedom, as compared to irrelevant heat-bath degrees of freedom, such as thermally randomized directions of individual atomic spins. In principle, one can incorporate the heat-bath in a very complicated Liouville operator, but this is neither practicable nor physically meaningful. A better approach is to describe the heat bath in terms of parameters such as temperature. Damping then implies increasing entropy and energy transfer from the relevant magnetic degrees of freedom to the heat bath.

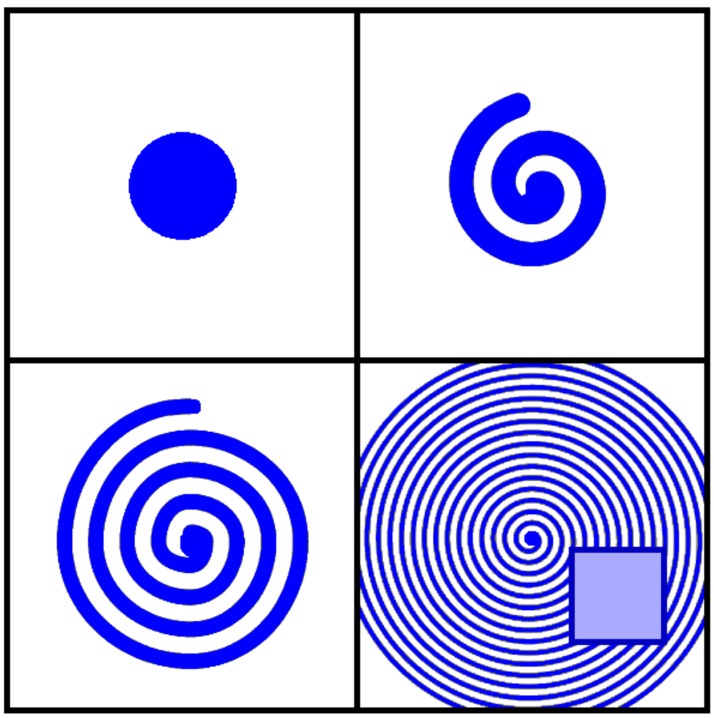

Fig. 2. Gibbs' ink parable. The stirring of a droplet of ink into leads to a distribution that is microscopically reversible but macroscopically irreversible. Simplifying somewhat, the microscopic view corresponds to the investigation of intrinsic magnetic properties, such as atomic magnetic moments, whereas the coarse-grained view corresponds to intrinsic properties, such as the local magnetization $\boldsymbol{M}(\boldsymbol{r})$.

3.2. Energy levels and irreversibility

Randomness of thermal or other origin yields irreversibility. Let us consider the very simple example of a noninteracting ensemble of precessing spins or nanoparticles described by the normalized magnetization

$$M(t) = \int p(\omega) \cos(\omega t)\, d\omega \tag{8}$$

where the distribution $p(\omega)$ obeys $\int p(\omega)\, d\omega = 1$. When all particles are identical, then they have a common precession frequency, $p(\omega) = \delta(\omega - \omega_0)$, and the precesssion is periodic, $M(t) = \cos(\omega_0 t)$. This limit corresponds to Eq. (4). However, particles encountered in reality are not identical, due to minor differences in structure, local magnetic fields, and/or heat-bath disorder. The integration in Eq. (9) then yields damped oscillations with exponential or nonexponential damping, depending on the distribution $p(\omega)$. For example, a distribution rectangular between $\omega_0 \pm \Delta\omega$ yields

$$M(t) = (\sin(\Delta\omega\, t)/\Delta\omega\, t) \cos(\omega_0\, t) \tag{9}$$

This function is shown in Fig. 3.

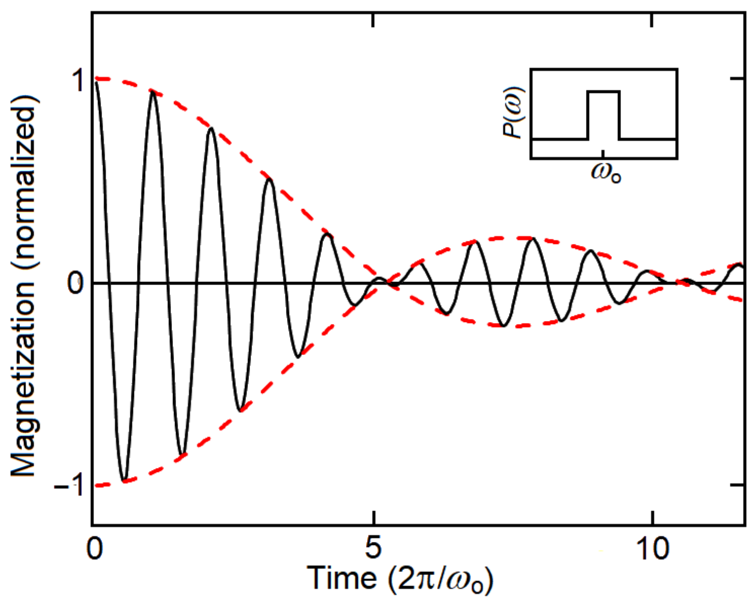

Fig. 3. A simple example of magnetic relaxation.

Equation (8) is semi phenomenological in the sense of assuming a distribution $p(\omega)$. More detailed calculations are demanding in various regards. First, the basic mechanisms responsible for relaxation, such as electron-magnon and electron-electron scattering tend to be very complicated [21-27]. For example, in metals there are quasiparticles whose life time increases with decreasing distance from the Fermi surface [28, 29]. Such quantum fluctuations are important in a variety of correlated and uncorrelated electron systems, as exemplified by quantum-phase transitions (QPT), quantum spin liquids (QSL), and non-Fermi liquids [23, 30, 31]. In §5.1, we will discuss one example, namely the antiferro-magnetic Heisenberg chain. Second, the inclusion of the heat bath creates a complicated damping behavior that is non-exponential for short times ('memory function') but typically exhibits a pronounced exponential tail [15, 16, 32].

3.3. Damped precession

A phenomenological approach to damping is replacing $\boldsymbol{H}$ in Eq. (5) by $\boldsymbol{H} - \tau_o \, \mathrm{d}\boldsymbol{M}/\mathrm{d}t$, which yields the Gilbert equation

$$\mathrm{d}\boldsymbol{M}/\mathrm{dt} = \gamma_G \, \boldsymbol{M} \times \boldsymbol{H} - \lambda_G \, \boldsymbol{M} \times \mathrm{d}\boldsymbol{M}/\mathrm{dt} \tag{10}$$

This equation, proposed around 1955 [33], was preceded by the Landau-Lifshitz equation [4]

$$\mathrm{d}\boldsymbol{M}/\mathrm{dt} = \gamma_L \, \boldsymbol{M} \times \boldsymbol{H} - \lambda_L \, \boldsymbol{M} \times (\boldsymbol{M} \times \boldsymbol{H}) \tag{11}$$

where the damping correction to $\boldsymbol{H}$ is $\boldsymbol{M} \times \boldsymbol{H}$ rather than $\mathrm{d}\boldsymbol{M}/\mathrm{d}t$. Both equations describe a damped spiral motion of the magnetization towards its equilibrium direction parallel to the field. Equation (11) exhibits the counterintuitive feature that the damping contribution $\mathrm{d}\boldsymbol{M}/\mathrm{dt}$ increases with the damping parameter λ_L. However, Eqs. (10-11) are equivalent with $\gamma_L = \gamma_G/(1 + \lambda_G{}^2 M_s{}^2)$ and $\lambda_L \, M_s = \gamma_L/(1 + \lambda_G{}^2 M_s{}^2)$, and one generally uses Eq. (11) while considering λ_G rather than λ_L as the physically relevant damping parameter [34]. This combination is commonly known as Landau-Lifshitz-Gilbert (LLG) equation.

A very transparent situation arises when $\boldsymbol{H} = H \, \boldsymbol{e}_z$, $\boldsymbol{M} \approx M_s \, \boldsymbol{e}_z$, and the damping is small. The perpendicular magnetization component $\boldsymbol{M}_\perp = M_x \, \boldsymbol{e}_x + M_y \, \boldsymbol{e}_y$ then undergoes a spiraling motion in the x-y-plane ($\omega = \gamma_o H$) and decays as $M_\perp(t) = M_\perp(0) \exp(-t/\tau)$, where $\tau = 1/\lambda_L M_s H$.

The cross product in the oscillation term has interesting micromagnetic consequences. Consider a Bloch wall lying in the y-z-plane, separating domains of magnetization parallel to the z-axis, and moved along the x-axis by a field in the z-direction. In the wall, the field acts on the y-component of the spins and creates a magnetization component in the x-direction. This leads to a demagnetizing field and causes the domain wall to exhibit an inertia proportional to $m \, \omega^2$, where the Döring mass m is about 1 μg/m^2 for Fe [35, 36]. This term becomes important at high frequencies. Domain-wall dynamics has attracted renewed attention in the context of race-track memories [37].

Electric currents, whose discussion goes beyond the scope of this paper, further complicate the situation but also offer new physics. A simple example is losses due to eddy currents in soft-magnetic materials [38] and various current-related relaxation mechanisms that are operative in the anomalous and spin Hall effects [39]. A topic of current interest is magnetic skyrmions moved by spin-polarized electric currents, a phenomenon described by the Landau-Lifshitz-Gilbert-Slonczewski and Thiele equations [18, 40].

4. Master, Fokker-Planck, and Langevin equations

The ink parable of Fig. 2 ignores diffusion effects and provides a deterministic description analogous to Eqs. (3-4). However, one can describe irreversible processes by using simplified versions of the Liouville operator. The idea is to separately consider relevant and heat-bath degrees of freedom, mapping the latter onto thermal noise and damping [16]. This yields probabilities $P(\boldsymbol{s}(\boldsymbol{r}), H, t)$, where $\boldsymbol{s}(\boldsymbol{r}) = \boldsymbol{M}(\boldsymbol{r})/M_s$ is the normalized magnetization, and averages such as $\langle \boldsymbol{s}(\boldsymbol{r}, H, t) \rangle$ [11, 16, 42, 43, 44, 45, 46].

4.1. Master equation

Let us start with a single magnetization variable $\boldsymbol{s} = s\,\mathbf{e}_z$ and consider transitions $W(s, s') = W(s' \rightarrow s)$. Equation (2) can then be approximated by the rate or *master* equation

$$\frac{\partial P(s)}{\partial t} = \int [W(s, s')\,P(s') - W(s', s)\,P(s)]\;\mathrm{d}s' \tag{12}$$

For transitions between discrete states s and s', the integral must be replaced by a sum. For two states, $s = \pm 1$ (or $\uparrow$ and $\downarrow$), Eq.(12) reduces to two equations $\mathrm{d}P_i/\mathrm{d}t = W_{ij}\,P_j - W_{ji}\,P_i$. Here

$$W_{ij} = \Gamma_o\,\exp\left(\frac{E_j - E_o}{k_B T}\right) \tag{13}$$

where we have assumed that the two states of energies $E_{\uparrow,\downarrow}$ are separated by an energy maximum E_o. Experiment shows that Γ_o is somewhat bigger than 10^9 Hz for many magnetic materials, corresponding to $1/\Gamma_o = \tau_o \lesssim 1$ ns [45, 47, 48].

Taking into account that $P_\uparrow + P_\downarrow = 1$ and $P_\uparrow - P_\downarrow = \langle s \rangle$ yields the following equation of motion

$$\frac{\mathrm{d}\langle s\rangle}{\mathrm{d}t} = \Gamma\,(s_o - \langle s\rangle) \tag{14}$$

Here $s_o = \tanh((E_\downarrow - E_\uparrow)/2k_B T)$ and the relaxation rate

$$\Gamma = \Gamma_o\exp\left(\frac{E_\uparrow - E_o}{k_B T}\right) + \Gamma_o\,\exp\left(\frac{E_\downarrow - E_o}{k_B T}\right) \tag{15}$$

When $|E_\uparrow - E_\downarrow| \gg k_B T$, then only one term survives, namely the one with the higher energy E_i, and $\Gamma = \Gamma_o\exp(-E_a/k_B T)$, where $E_a = E_o - E_i$ has the character of an energy barrier. In terms of relaxation times $\tau = 1/\Gamma$,

$$\tau = \tau_o\exp\left(\frac{E_a}{k_B T}\right) \tag{16}$$

This equation governs the slow dynamics of magnetization processes (§6).

4.2. Fokker-Planck and Langevin equations

A major simplification of the master equation is achieved by assuming that s and s' differ by a small amounts only. Series expansion then transforms the integral in Eq. (12) into a differential equation known as the *Fokker-Planck equation*. For a single but continuous spin,

$$\frac{\partial P}{\partial t} = \frac{\Gamma_o}{k_B T}\,\frac{\partial}{\partial s}\left(\frac{\partial E}{\partial s}\;P\right) + \Gamma_o\,\frac{\partial P^2}{\partial s^2} \tag{17}$$

The Fokker-Plack equation can be considered a generalized diffusion equation in spin space.

Putting $\partial P/\partial t = 0$ in Eq. (17) and integrating over s shows that the Fokker-Planck equation reproduces the correct equilibrium limit $P \sim \exp(-E(s)/k_B T)$. In the opposite limit of nonequilibrium states captured in deep potential valleys, with activation energies E_a much larger than $k_B T$, the dynamics approaches the Arrhenius limit with relaxation times $\tau_o \exp(E_a/k_B T)$. In chemistry, this limit is known as Kramers' escape-rate theory (1940), but in magnetism, it is more frequently referred to as Arrhenius-Brown-Néel theory. This theory differs from Eq. (13-16) by considering continuous spin variables s, not only $s = \pm 1$, but yields the same relaxation behavior for deep potential minima.

Once the probability $P(s, t)$ is known, $\langle s(t) \rangle$ and $\langle s(t)s(t') \rangle$ are obtained by straightforward integration, but it is sometimes easier to determine $s(t)$ directly, using the *Langevin equation*

$$\frac{\partial s}{\partial t} = - \frac{\Gamma_o}{k_B T} \frac{\partial E}{\partial s} + \sqrt{2\Gamma_o}\, \xi(t) \tag{18}$$

Here $\xi(t)$ is a random thermal force that has the character of delta-correlated white noise obeying $\langle \xi(t) \rangle = 0$ and $\langle \xi(t)\, \xi(t') \rangle = \delta(t - t)$ [11, 44, 45].

5. Spin-wave dynamics

Equations (5, 10, 11) describe the dynamics of magnetization vectors of constant magnitude, $M_x^2 + M_y^2 + M_z^2 = M_s^2$, so that the dynamics is described by two equation for two independent magnetization variables. When $\boldsymbol{M}(\boldsymbol{r}) \approx M_s\, \boldsymbol{e}_z$, realized for example by easy-axis anisotropy, the equations of motion can be linearized with respect to M_x and M_y. The time evolution of M_x and M_y has then the character of spin waves (magnons) of wave vector k and angular frequency ω. Since the uniform mode ($k = 0$) was discussed in §3.3, the focus of this section is on wave dispersion relation $\omega(\boldsymbol{k})$, which was first considered by Bloch [3].

5.1. Quantum-mechanics of magnons

The dispersion relation $\omega(\boldsymbol{k})$ of ferromagnetic spin waves is quasi-classical (§5.2), but magnons in antiferromagnets involve nontrivial quantum mechanics [22, 49] and their classical description (§5.3) is rather crude. In good approximation, the interaction between neighboring spins is Heisenberg exchange $-2\,J\, \mathbf{S}\cdot\mathbf{S}'$. It is convenient to introduce rising and lowering operators $S^\pm$ so that $S^x = (S^+ + S^-)/2$ and $S^y = (S^+ - S^-)/2i$. Evaluation of $\mathbf{S}\cdot\mathbf{S}'$ shows that the ladder operators $S^\pm$ exchange spins in a literary sense, whereas S^z is trivial in the sense that it merely counts the ↑ and ↓ spins.

An infinite ferromagnetic spin chain has the ground state |↑↑↑↑↑↑>, corresponding to $k = 0$. However a single reversed spin, for example |↑↑↓↑↑↑>, is not an eigenfunction of the Hamiltonian, because the ladder operators produce spin configurations such as |↑↑↑↓↑↑>. Eigenstates are created by superposing localized spin flips with coefficients $\exp(i\,k\,a)$, and the corresponding spin waves (magnons) have energies $2J(1 - \cos(ka))$ [3].

The behavior of antiferromagnets (AFM) is much more complicated. Intuitively, one would expect a quasi-classical ground state of the type |↑↓↑↓↑↓> or |↓↑↓↑↓↑>. However, neither of these two Néel states nor any combination of them are eigenstates of the AFM Hamiltonian [22]. The ground state and the low-lying excited states are superpositions of Bethe wave functions with nanoscale spin correlations [49].

The complicated behavior of Heisenberg antiferromagnets is a *correlation effect*. By definition, the Heisenberg model is a strongly correlated model, and in antiferromagnets, ↓ spins are able to hop onto sites with ↑ spins and *vice versa*. This hopping is suppressed in ferromagnets, because ↑ spins are disallowed by the Pauli principle to hop onto neighboring ↑ sites. As thermodynamic fluctuations, quantum fluctuations are most pronounced in low-dimensional solids [23, 49], but they also yield corrections in three-dimensional magnets [50].

5.2. Spin-wave dispersion

Let us assume a ferromagnet where x and y are equivalent and $\boldsymbol{M} \approx M_z\, e_z$, so that Eq. (4) yields $\omega = \gamma_o H$ for $k = 0$. The treatment of nonzero wave vectors requires the explicit consideration of interatomic exchange, described by the exchange stiffness A. Expressing the magnetization component in the x-y-plane $\boldsymbol{m} = (M_x\, \boldsymbol{e}_x + M_y\, \boldsymbol{e}_y)/M_s$ yields the Zeeman energy density $E/V = ½\, \mu_o M_s H m^2$, where we assume that $\boldsymbol{H} = H\, \mathbf{e}_z$. Similar expansions can be made for the exchange and anisotropy energies [45], leading to

$$E/V = A\,(\nabla m)^2 + K_1(\boldsymbol{r})\, m^2 + ½\, \mu_o M_s H\, m^2 \tag{19}$$

The eigenvalues of this quadratic form determine the resonance frequencies. We see that K_1 additively modifies the field and that A does so after Fourier transformation. For $K_1(\boldsymbol{r}) = const.$, the dispersion relation is

$$\omega(\boldsymbol{k}) = \gamma_o\,(H + 2K_1/\mu_o M_s + 2A\boldsymbol{k}^2/\mu_o M_s) \tag{20}$$

Spin waves are deviations from perfect spin alignment, so that thermally activated spin waves of energy $\hbar\,\omega$ reduce the spontaneous magnetization Ms. The spontaneous magnetization Ms is defined by the formal limit H = 0. For isotropic magnets ($K_1 = 0$), integration over all thermal spin-wave excitations yields [22]

$$M_s(0) - M_s(T) \sim T^{d/2} \int k^{3-d}\, \mathrm{d}k \tag{21}$$

where d is the dimensionality of the magnet and the integral extends from $k = 0$ to $k \approx \pi/a$, where a is the interatomic distance.

In three dimensions, Eq. (21) is Bloch's $T^{3/2}$ law for the temperature dependence of the magnetization [3]. For $d \leq 2$, the integral exhibits an infrared (small k) divergence and $M_s(T) = 0$ at all nonzero temperatures, meaning that $T_c = 0$ [22]. *Anisotropic magnets* ($K_1 > 0$) have a spin-wave anisotropy gap $H = 0$ and $k = 0$. The gap is insufficient to create ferromagnetism in one dimension but yields $k_B T_c \sim J/\ln(J/K_1)$ in two dimensions, where the divergence is logarithmically weak [51].

Nanoscale confinement and structural inhomogeneity also affects the magnon's energy levels [45, 52]. For example, a magnet may contain regions of different hardness, described by an anisotropy distribution $K_1(\boldsymbol{r})$. In this case, the quadratic form (19) is no longer diagonalized by Fourier transformation, because $K_1(\boldsymbol{r})$ mixes different spin waves $\boldsymbol{k}$ and $\boldsymbol{k}'$. The diagonalization then requires the solution of a nontrivial differential equation [45, 53, 54]. In the context of surface magnetism, these spin-waves modes are known as Damon-Eshbach modes [55].

5.3. Antiferromagnetic spin waves

In frequency units, H and K_1 are of the order of several GHz, and the same is true for Dzyaloshinski-Moriya interactions and for *nanoscale* exchange contributions. However, the exchange contribution becomes very large, of the order of several THz, when the spin-wave periodicity $2\pi/k$ is comparable to the interatomic distance $a \approx 0.25$ nm. Such spin-wave modes exist in antiferromagnets, and there are efforts to exploit them for THz information processing [9].

Figure 4 shows an A-B two-sublattice magnet having $\boldsymbol{M}_A \approx -\boldsymbol{M}_B$ and $|\boldsymbol{M}_A| = |\boldsymbol{M}_B| = M_o$. The model includes both antiferromagnets (a), where A and B are chemically and crystallographically equivalent, and compensated ferrimagnets (b), where A and B are chemically and/or crystallographically different. Micromagnetic sublattice anisotropies and sublattice exchange interactions are well-defined and easily incorporated into micromagnetic calculations [56, 57, 58]. Note that this micromagnetic approach is a fairly crude approximation, because it ignores AFM quantum fluctuations (§5.1). These fluctuations are particularly important in ultathin films and pose an additional challenge in THz information processing.

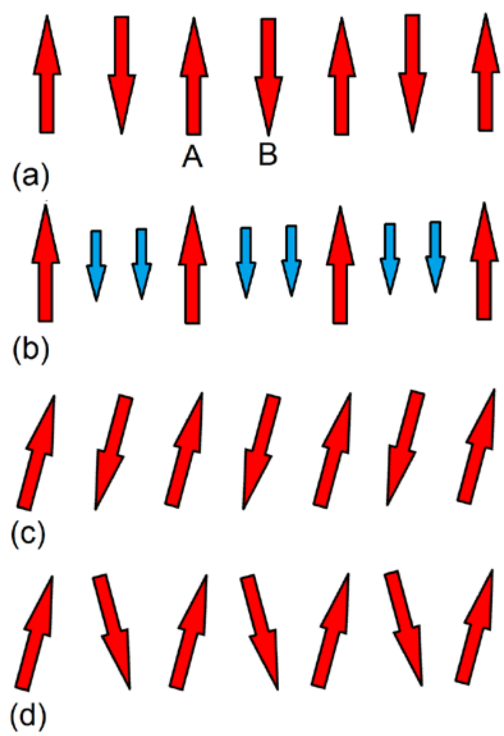

Fig. 4. Antiferromagnetic spin dynamics: (a) antiferromagnet, (b) compensated ferrimagnets, (c) coherent rotation of the Néel vector is rotating, and (d) THz mode.

Let us restrict the consideration to $k = 0$, that is, the spins remain parallel in each sublattice. The model of Fig. 4 then has two basic magnetization modes, namely (c) and (d). Let us denote the deviations from $\boldsymbol{M}_A = +M_o\, \boldsymbol{e}_z$ and $\boldsymbol{M}_B = -M_o\, \boldsymbol{e}_z$ by m_A and m_B, respectively, both defined clockwise in the x-z-plane. In (c), $m_B = m_A$, whereas in (d), $m_B = -\, m_A$. Equation (19) now becomes

$$E \sim K_A\, m_A^2 + K_B\, m_B^2 + J_{AB}\, (m_A - m_B)^2 \tag{22}$$

The resonance frequencies are the eigenvalues of the 2×2 matrix

$$\omega = \frac{1}{\gamma_o} \begin{pmatrix} K_A & J_{AB} \\ J_{AB} & K_B \end{pmatrix} \tag{23}$$

where $K_{A/B}$ and J_{AB} must be interpreted as anisotropy and exchange fields, respectively.

In the AFM case, Figs. 4(a, c, d), the two sublattice anisotropies are equal, $K_A = K_B = K$. The two eigenmodes are then exactly those shown in the figure, namely $m_1 = (1, 1)\, m_o$ for (c) and $m_2 = (1, -1)\, m_o$ for (d), where m_o is the mode amplitude. The resonance frequencies are $\omega_1 = K/\gamma_0$ (GHz) and $\omega_2 = (J_{AB} + K)/\gamma_0$ (THz). The physical explanation is that the mode m_1 (c) rotates the Néel vector $\boldsymbol{M}_A - \boldsymbol{M}_B$ but leaves the relative spin angles unchanged, so that the effective field is equal to the relatively small anisotropy field. By contrast, m_2 (d) changes the angle between neighboring spins, which corresponds to huge exchange fields.

With respect to information processing, the challenge is the writing and reading of the information, that is, the excitation and detection of spin waves. The mode of Fig. 4(d) can be excited by a homogeneous magnetic field, but the corresponding amplitude is very small $m_o \approx H/J_{AB}$. The mode of Fig. 4(c) cannot be excited by a homogenous field at all and requires specific excitations mechanisms, such as staggered magnetic fields $H \sim \cos(\pi x/a)$, which are difficult to realize in practice, or specific excitation mechanisms, involving for example Dzyaloshinski-Moriya interactions [59]. However, the main disadvantage of modes that change the Néel vector (c) is their low frequency.

In various regards, compensated ferrimagnets are superior to simple antiferromagnets. For example, subjecting the structure of Fig. 4(b) to spin-polarized currents is likely to affect the sublattices differently, making is possible to change Néel vectors and to measure them through magnetoresistance.

6. Slow magnetization dynamics

Equations (10-11) describe the viscous relaxation into a local energy minimum, which is only one aspect of nonequilibrium magnetism. In reality, the approach to equilibrium involves thermally activated jumps over energy barriers, as discussed in §4.2. This mechanism dominates the slow magnetization dynamics of permanent magnets, soft magnets, magnetic recording media, spin glasses, ferrofluids, and magnetic rocks [44, 60, 61, 62, 63, 64, 65]. For example, freshly magnetized permanent magnets lose a few mT of their magnetization within the first few hours (magnetic viscosity). Magnetic viscosity was explained by Becker and Döring in 1939 as a superposition of exponential relaxation events [5] and microscopically explained in terms of energy barriers by Néel in 1949 [66].

Energy barriers normally obey $E_a \gg k_B T$, so that one can apply Kramers' escape rate theory [67], which leads to Eq. (16). In addition to the leading energy dependence of τ, there is an effect due to activation *entropy* S_a [68]. Replacing E_a by $F_a = E_a - T S_a$ changes τ_o to $\tau_o \exp(-S_a/k_B)$.

6.1. Magnetic viscosity and sweep-rate dependence of coercivity

Let us assume that the local magnetization process described by τ completely reverses the magnetization, so that

$$M(t) = -M_s + 2 M_s \exp(-t/\tau) \tag{24}$$

In reality, there is always an energy-barrier distribution $P(E_a)$ due to real-structure features such as structural inhomogeneities and local magnetic fields. It is therefore necessary to average over this distribution:

$$M(t) = -M_s + 2 M_s \int_{-\infty}^{\infty} P(E_a)\, e^{-(t/\tau_o)\exp(-E_a/k_B T)}\, dE_a \tag{25}$$

Next we exploit that $\alpha \exp(\beta E) = \exp(\beta E + \ln\alpha)$ and $\exp(-\exp(-x/\varepsilon)) \approx \Theta(x)$, where $\varepsilon = k_B T/E \ll 1$ and $\Theta(x)$ is the step function, equal to 0 and to 1 for $x < 0$ and $x > 0$, respectively. Putting these relations into Eq. (25) yields the *magnetic-viscosity law*

$$M(H, t) = M(H, t_o) - S \ln(t/t_o) \tag{26}$$

where the magnetic-viscosity constant $S = 2 k_B T \; \mathrm{P}(0)\, \mathrm{M_s}$. The superposition character of logarithmic time dependence was phenomenologically understood by 1939 [5]. Later research improved the description of the limits $t = 0$ and $t = \infty$, where the logarithm diverges [70].

A related phenomenon is the time dependence (sweep-rate dependence) of the coercivity. Stoner-Wohlfarth particles, where the magnetization reversal proceeds by uniform (coherent) rotation, are characterized by the energy barrier

$$E_a(H) = K_1 V_o \left(1 - \frac{H}{H_o}\right)^{\mathrm{m}} \tag{27}$$

where V_o is the particle volume and $H_o \sim 2K_1/\mu_o M_s$. In the absence of thermal excitations ($E_a = 0$), the coercivity is equal to H_o. Combination of Eqs. (16) and (27) yields

$$H_c = H_o \left(1 - \left(\frac{k_B T}{K_1 V_o} \ln(\tau/\tau_o)\right)^{1/\mathrm{m}}\right) \tag{28}$$

This relation was first derived by Kneller in 1966 [47] and is known as the Sharrock equation in the magnetic-recording community.

Generalized to other systems, the exponent m in Eqs. (27-28) can take values of 2 or 3/2. The exponent $m = 2$ describes aligned easy-axis particles (c-axis parallel to the magnetic field), whereas $m = 3/2$ describes low-symmetry systems, such misaligned particles [45]. The exponent $m = 3/2$ was first derived by Néel [69] for domain-wall motion but can be derived very generally [45]. Other exponents, such as $m = 1$ sometimes assumed for Zeeman interaction, are unphysical in the low-temperature limit considered here.

Superparamagnetic particles are characterized by rapid magnetization decays, because K_1V_o is no longer much larger than k_BT. Defining superparamagnetism by a waiting time of $\tau = 100$ s and using Eq. (16) yields the zero-field stability condition $K_1V_o/k_BT \geq 25$, corresponding to a room-temperature energy-barrier height of 7,500 K. The quantity $K_1V_o/k_BT = \xi$ is referred to as the *stability parameter*. Thermal stability over 10 years corresponds to $\xi = 40$, whereas error considerations in recording media require stability parameters in excess of 60 [63].

6.2. *Onset of ferromagnetism*

As we have seen in §5.2, there is no ferromagnetism in one-dimensional magnets. This finding is seemingly at odds with the experimental ferromagnetism in magnetic wires. The paradox is solved by considering equilibration times [71]. Figure 5 illustrates how the ferromagnetic long-range order of an infinite anisotropic spin chain (a) is easily destroyed by thermal excitations (b). The creation of a domain requires a finite activation energy E_a and may take a long time according to Eq. (16). However, this time is always finite for nonzero temperatures T.

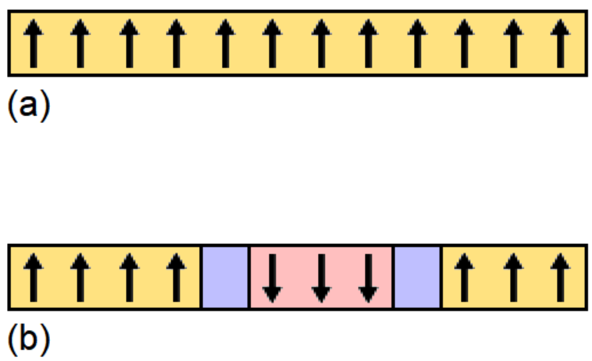

Fig. 5. Slow dynamics in a one-dimensional magnet: (a) ferromagnetic initial state and (b) decay of average magnetization due to thermally activated domains.

In practice, time is an important consideration. A few seconds or minutes are typically sufficient to perform a magnetization measurement, and the spin structure of the wires in 100 or 1000 years is experimentally irrelevant. For a wire having a square cross section D^2, the energy of the two domains in Fig. 5(b) is $E_a = 8D^2(AK_1)^{1/2}$. Taking $\tau_o = 1$ ns, $A = 10$ pJ/m, $K_1 = 1$ MJ/m^3, and square cross sections of area D^2 yields times of about 0.5 μs for $D = 1$ nm, 40 s for $D = 2$ nm, and 20 million years for $D = 3$ nm. This example epitomizes the transition from atomic-scale magnetism to nanoscale at feature sizes of a very few nanometers.

7. Conclusions

In summary, we have outlined how quantum-mechanical and nanoscale effects combine to yield new and interesting physics. Some findings from the first decades of the 20th century appear in a completely new light, such as the Berry-phase interpretation of spin rotation and the non-cloning implications of entangled spins. In some cases, magnetization dynamics provides an intuitive access to complicated problems, for example to the onset of ferromagnetism in low-dimensional systems. Many phenomena are waiting to be explored and exploited in the medium to far future, such as quantum computing and terahertz information processing using magnetic degrees of freedom.

Acknowledgement

This research is supported by DOE BES (DE-FG02-04ER46152 and NCMN.

References

[1] J. A. Ewing and H. G. Klaassen, "Magnetic qualities of Fe", Phil. Trans. Roy. Soc., **184**A, 985-1039 (1893).

[2] A. Mühlbauer, "History of Induction Heating and Melting", Vulkan-Verlag, Essen 2008.

[3] F. Bloch, "Zur Theorie des Ferromagnetismus", Z. Phys. **61** (1930) 206-219.

[4] L. Landau and E. Lifshitz, "On the theory of the dispersion of magnetic permeability in ferromagnetic bodies", Phys. Z. Sowjetunion, **8** (1935) 153-169.

[5] R. Becker and W. Döring, *Ferromagnetismus,* Springer, Berlin 1939.

[6] M. V. Berry, "Quantal phase factors accompanying adiabatic changes", Proc. R. Soc. Lond. A **392**, 45-57 (1984).

[7] W. Wootters and W. Zurek, "A Single Quantum Cannot be Cloned". Nature. **299**, 802–803 (1982).

[8] G. C. Ghirardi and T. Weber, "Quantum mechanics and faster-than-light communication: Methodological considerations", Nuovo Cim. B **78**, 9-20 (1983).

[9] Ch. Song, Y. You, X. Chen, X. Zhou, Y. Wang, and F. Pan, "How to manipulate magnetic states of antiferromagnets", Nanotechnology **29**, 112001-1-20 (2018).

[10] R. Skomski, H.-P. Oepen, and J. Kirschner, "Micromagnetics of ultrathin films with perpendicular magnetic anisotropy", Phys. Rev. B **58**, 3223-3227 (1998).

[11] R. Skomski, *Simple Models of Magnetism*, University Press, Oxford (2008).

[12] C. Kittel, *Introduction to Solid-State Physics*, Wiley, New York 1986.

[13] M. Farle, "Ferromagnetic Resonance of Ultrathin Metallic Layers", Rep. Prog. Phys. **61**, 755-826 (1998).

[14] L. R. Walker, "Magnetostatic Modes in Ferromagnetic Resonance", Phys. Rev. **105**, 390–399 (1957).

[15] W. Brenig, *Statistical theory of heat: Nonequilibrium phenomena*, Springer, Berlin 1989.

[16] R. Zwanzig, *Nonequilibrium Statistical Mechanics*, University Press, Oxford 2001.

[17] D. Xiao, M.-Ch. Chang, and Q. Niu, "Berry phase effects on electronic properties", Rev. Mod. Phys. **82**, 1959–2007 (2010).

[18] Sh. Seki and M. Mochizuki, "Skyrmions in Magnetic Materials", Springer International, Cham 2016.

[19] R. Skomski and D. J. Sellmyer, "Nonadiabatic Berry phase in nanocrystalline magnets", AIP Adv. **7**, 055802-1-4 (2017).

[20] M. A. Nielsen and I. L. Chuang, *Quantum Computation and Quantum Information*, University Press, Cambridge 2000.

[21] D. M. Edwards, J. A. Hertz, "Electron-magnon interactions in itinerant ferromagnetism: I. Formal theory", J. Phys. F: Met. Phys. **3**, 2174-2190 (1973).

[22] N. W. Ashcroft and N. D. Mermin, Solid State Physics, Saunders, Philadelphia 1976.

[23] A. J. Schofield, "Non-Fermi liquids", Contemporary Phys. **40**, 95-115 (1999).

[24] A. A. Starikov, P. J. Kelly, A. Brataas, Y. Tserkovnyak, and G. E. W. Bauer, "Unified First-Principles Study of Gilbert Damping, Spin-Flip Diffusion, and Resistivity in Transition Metal Alloys", Phys. Rev. Lett. **105**, 236601-1-4 (2010).

[25] M. Fähnle and C. Illg, "Electron theory of fast and ultrafast dissipative magnetization dynamics", J. Phys.: Condens. Matter **23**, 493201-1-18 (2011).

[26] V. Kambersky and C. E. Patton, "Spin-wave relaxation and phenomenological damping in ferromagnetic resonance", Phys. Rev. B **11**, 2668–2672 (1975).

[27] H. Suhl, "Theory of the magnetic damping constant", IEEE Trans. Magn. **34** (4), 1834-1838 (1998).

[28] S. Doniach and S. Engelsberg, "Low-Temperature Properties of Nearly Ferromagnetic Fermi Liquids", Phys. Rev. Lett. **17**, 750-753 (1966).

[29] W. Jones and N. H. March, *Theoretical Solid State Physics I*, Wiley & Sons, London 1973.

[30] J. A. Hertz, "Quantum critical phenomena", Phys. Rev. B **14**, 1165-1184 (1976).

[31] Q. Si, S. Rabello, K. Ingersent, and J. L. Smith, "Locally critical quantum phase transitions in strongly correlated metals", Nature **413**, 804-808 (2001).

[32] R. Zwanzig, "Memory effects in irreversible thermodynamics", Phys. Rev. **124** (1961) 983-992.

[33] T. L. Gilbert, "Classics in Magnetics A Phenomenological Theory of Damping in Ferromagnetic Materials", IEEE Trans. on Magn. **40** (6), 3443-3449 (2004).

[34] H. Kronmüller u. M. Fähnle, *Micromagnetism and the Microstructure of Ferromagnetic Solids*, University Press, Cambridge 2003.

[35] W. Döring, "Über die Trägheit der Wände zwischen Weißschen Bezirken", Z. Naturforsch. **3**a, 373-379 (1948).

[36] S. Chikazumi, *Physics of Magnetism*, Wiley, New York 1964.

[37] S. S. P. Parkin, M. Hayashi, and L. Thomas, "Magnetic Domain-Wall Racetrack Memory", Science **320**, 190-194 (2008)

[38] R. M. Bozorth, *Ferromagnetism*, van Nostrand, Princeton, New Jersey, 1951.

[39] N. Nagaosa, J. Sinova, Sh. Onoda, A. H. MacDonald, and N. P. Ong, "Anomalous Hall effect", Rev. Mod. Phys. **82**, 1539-1592 (2010).

[40] N. Nagaosa and Y. Tokura, "Topological properties and dynamics of magnetic skyrmions", Nature Nanotechnology **8**, 899-911 (2013).

[41] W. Jiang, P. Upadhyaya, W. Zhang, G. Yu, M. B. Jungfleisch, F. Y. Fradin, J. E. Pearson, Y. Tserkovnyak, K. L. Wang, O. Heinonen, S. G. E. te Velthuis, A. Hoffmann, "Blowing magnetic skyrmion bubbles", Science **349**, 283-286 (2015).

[42] H. Haken, *Synergetics*, Springer, Berlin 1977.

[43] W. F. Brown, "Thermal fluctuations of a single-domain particle", Phys. Rev. **130**, 1677-1686 (1963).

[44] K.-H. Fischer and A. J. Hertz, *Spin Glasses*, University Press, Cambridge 1991.

[45] R. Skomski, "Nanomagnetics", J. Phys.: Condens. Matter **15**, R841-896 (2003).

[46] R. Dittrich, T. Schrefl, D. Suess, W. Scholz, H. Forster, and J. Fidler, "A path method for finding energy barriers and minimum energy paths in complex micromagnetic systems", J. Magn. Magn. Mater. **250**, 12-19 (2002).

[47] E. Kneller, "Theorie der Magnetisierungskurve kleiner Kristalle", in: *Handbuch der Physik XIII/2: Ferromagnetismus*, Ed.: H. P. J. Wijn, Springer 1966, pp. 438-544.

[48] R. Skomski, J. Zhou, and D. J. Sellmyer, "Relaxation in Magnetic Nanostructures", J. Appl. Phys. **97**, 10A702-1-3 (2005).

[49] M. Karbach and G. Müller, "Introduction to the Bethe ansatz I", Computers in Physics **11**, 36-44 (1997).

[50] R. Skomski, P. Kumar, B. Balamurugan, B. Das, P. Manchanda, P. Raghani, A. Kashyap, and D. J. Sellmyer, "Exchange and magnetic order in bulk and nanostructured Fe_5Si_3", J. Magn. Magn. Mater. **460**, 438-447 (2018).

[51] M. Bander and D. L. Mills, "Ferromagnetism of Ultrathin Films", Phys. Rev. B **38** (1988) 12015-12018.

[52] Hillebrands, B., and K. Ounadjela (Eds.), *Spin Dynamics in Confined Magnetic Structures I*, Springer, Berlin, 2002.

[53] M. I. Chipara, R. Skomski, and D. J. Sellmyer, "Magnetic Modes in Ni Nanowires", J. Magn. Magn. Mater. **249**, 246-250 (2002).

[54] R. Skomski, M. Chipara, and D. J. Sellmyer, "Spin-wave modes in magnetic nanowires", J. Appl. Phys. **93**, 7604-7606 (2003).

[55] J. R. Eshbach and R. W. Damon, "Surface Magnetostatic Modes and Surface Spin Waves", Phys. Rev. **118** (1960) 1208-1210.

[56] F. Keffer, H. Kaplan, and Y. Yafet, "Spin Waves in Ferromagnetic and Antiferromagnetic Materials", Am. J. Phys. **21**, 250-257 (1953).

[57] A. I. Akhiezer, V. G. Bar'yakhtar, and M. I. Kaganov, "Spin waves in ferromagnets and antiferromagnets. I" Soviet Physics Uspekhi **3**, 567–592 (1961).

[58] J. Richter and R. Skomski, "Antiferromagnets with random anisotropy", phys. stat. sol (b) **153**, 711-719 (1989).

[59] L. Hao, D. Meyers, H. Suwa, J. Yang, C. Frederick, T. R. Dasa, G. Fabbris, L. Horak, D. Kriegner, Y.Choi, J.-W. Kim, D. Haskel, P. J. Ryan, H. Xu, C. D. Batista, M. P. M. Dean, and J. Liu, "Giant magnetic response of a two-dimensional antiferromagnet", Nature Physics **14**, 806–810 (2018).

[60] R. Skomski and J. M. D. Coey, *Permanent Magnetism*, Institute of Physics, Bristol 1999.

[61] J. L. Dormann, L. Bessais, and D. Fiorani, "A dynamic study of small interacting particles: superparamagnetic model and spin-glass laws", J. Phys. C **21**, 2015-2034 (1988).

[62] G. W. D. Spratt, P. R. Bissell, and R. W. Chantrell, "Static and dynamic experimental studies of particulate recording media", J. Magn. Magn. Mater. **75** (1988) 309-318 (1988).

[63] D. J. Sellmyer, M. Yu, R. A. Thomas, Y. Liu, and R. D. Kirby, "Nanoscale design of films for extremely high density magnetic recording", Phys. Low-Dim. Struct. **1-2**, 155-165 (1998).

[64] E. P. Wohlfarth, "The coefficient of magnetic viscosity", J. Phys. F: Met. Phys. 14 L155-159 (1984).

[65] J. M. Coey, *Magnetism and Magnetic Materials*, University Press, Cambridge 2010.

[66] L. Néel, "Théorie du trainage magnétique des ferromagnétiques en grains fins avec applications aux terres cuites", Ann. Géophys. **5**, 99-136 (1949).

[67] H. A. Kramers, "Brownian motion in a field of force and the diffusion model of chemical reactions", Physica **7**, 284-304 (1940).

[68] R. Skomski, R. D. Kirby, and D. J. Sellmyer, "Activation Entropy, Activation Energy, and Magnetic Viscosity", J. Appl. Phys. **85**, 5069-5071 (1999).

[69] L. Néel, "Le traînage magnétique des substances massives dans le domaine de Rayleigh", J. de Phys. Rad. 11, 49-61 (1950).

[70] R. Skomski and V. Christoph, "Power law behaviour of magnetic viscosity", phys. stat. sol. (b) **156**, K149-152 (1989).

[71] J. Shen, R. Skomski, M. Klaua, H. Jenniches, S. S. Manoharan, and J. Kirschner, "Magnetism in One Dimension: Fe on Cu(111)", Phys. Rev. B **56** (1997) 2340-2343.